

University of Windsor

Scholarship at UWindor

Electronic Theses and Dissertations

Theses, Dissertations, and Major Papers

1-1-2007

FEA-aided design of a special tensile specimen for steel during quenching.

Chao Zheng
University of Windsor

Follow this and additional works at: <https://scholar.uwindsor.ca/etd>

Recommended Citation

Zheng, Chao, "FEA-aided design of a special tensile specimen for steel during quenching." (2007).
Electronic Theses and Dissertations. 7177.
<https://scholar.uwindsor.ca/etd/7177>

This online database contains the full-text of PhD dissertations and Masters' theses of University of Windsor students from 1954 forward. These documents are made available for personal study and research purposes only, in accordance with the Canadian Copyright Act and the Creative Commons license—CC BY-NC-ND (Attribution, Non-Commercial, No Derivative Works). Under this license, works must always be attributed to the copyright holder (original author), cannot be used for any commercial purposes, and may not be altered. Any other use would require the permission of the copyright holder. Students may inquire about withdrawing their dissertation and/or thesis from this database. For additional inquiries, please contact the repository administrator via email (scholarship@uwindsor.ca) or by telephone at 519-253-3000ext. 3208.

**FEA-AIDED DESIGN OF A SPECIAL
TENSILE SPECIMEN FOR STEEL
DURING QUENCHING**

by

Chao Zheng

A Thesis
Submitted to the Faculty of Graduate Studies
through Engineering Materials
in Partial Fulfillment of the Requirements for
the Degree of Master of Applied Science at the
University of Windsor

Windsor, Ontario, Canada

2007

© 2007 Chao Zheng



Library and Archives
Canada

Published Heritage
Branch

395 Wellington Street
Ottawa ON K1A 0N4
Canada

Bibliothèque et
Archives Canada

Direction du
Patrimoine de l'édition

395, rue Wellington
Ottawa ON K1A 0N4
Canada

Your file *Votre référence*
ISBN: 978-0-494-80238-0
Our file *Notre référence*
ISBN: 978-0-494-80238-0

NOTICE:

The author has granted a non-exclusive license allowing Library and Archives Canada to reproduce, publish, archive, preserve, conserve, communicate to the public by telecommunication or on the Internet, loan, distribute and sell theses worldwide, for commercial or non-commercial purposes, in microform, paper, electronic and/or any other formats.

The author retains copyright ownership and moral rights in this thesis. Neither the thesis nor substantial extracts from it may be printed or otherwise reproduced without the author's permission.

In compliance with the Canadian Privacy Act some supporting forms may have been removed from this thesis.

While these forms may be included in the document page count, their removal does not represent any loss of content from the thesis.

AVIS:

L'auteur a accordé une licence non exclusive permettant à la Bibliothèque et Archives Canada de reproduire, publier, archiver, sauvegarder, conserver, transmettre au public par télécommunication ou par l'Internet, prêter, distribuer et vendre des thèses partout dans le monde, à des fins commerciales ou autres, sur support microforme, papier, électronique et/ou autres formats.

L'auteur conserve la propriété du droit d'auteur et des droits moraux qui protègent cette thèse. Ni la thèse ni des extraits substantiels de celle-ci ne doivent être imprimés ou autrement reproduits sans son autorisation.

Conformément à la loi canadienne sur la protection de la vie privée, quelques formulaires secondaires ont été enlevés de cette thèse.

Bien que ces formulaires aient inclus dans la pagination, il n'y aura aucun contenu manquant.


Canada

ABSTRACT

Quenching is the most effective way to strengthen steel. By cooling steel rapidly enough from an austenitizing temperature to room temperature, a hard and strong phase called martensite is formed from soft austenite. Considerable previous research work has been dedicated to characterize this process, and computer simulation programs have been developed to capture the phase transformation and dimensional change evolution as a function of temperature in the quenching process. Among the successful commercial applications is the prediction of residual stress and distortion brought about by the quenching process, which acts as a guide to optimize the quenching process. But how to measure mechanical properties, which have a nonlinear temperature and microstructure dependence and which are needed to conduct an accurate simulation, remains the most challenging problem to solve. This thesis reveals a special and unique kind of resistance heated specimen which has been designed to measure the nonlinear mechanical properties of tool steels by tensile testing, during each stage of the entire process of quenching.

DEDICATION

To my wife Qi and daughter Gloria

ACKNOWLEDGEMENTS

First of all, I would like to express my gratitude to my academic advisor, Dr. Daniel F. Watt, for his help throughout this research program. From his comprehensive knowledge and deep insight in materials science and engineering derives the idea of launching this challenging research program. His detailed guidance, constructive suggestion and involvement ensured the successful completion of this program.

I would also like to thank BOHLER UDDEHOLM LIMITED for their generous donation of research materials for this program. Help from many of the technicians in Central Technical Research, especially Gangyong Zhang and Andy Jenner for their development of our experimental device and machining of our samples, are also highly appreciated.

Funding for this research program and financial support in the form of research assistantship from Dr. Daniel F. Watt's funding provided by Natural Sciences and Engineering Research Council of Canada (NSERC), and from his personal funds, is especially acknowledged and greatly appreciated.

Further acknowledgement should go to the Province of Ontario, Canada for the financial support through the Ontario Graduate Scholarship (OGS) and also to the University of Windsor for financial support in the form of Graduate Assistantships and partial tuition waiving.

TABLE OF CONTENTS

ABSTRACT	iii
DEDICATION	iv
ACKNOWLEDGEMENTS	v
TABLE OF CONTENTS	vi
LIST OF FIGURES	viii
LIST OF TABLES	xii
CHAPTER 1 INTRODUCTION	1
1.1 Motivation.....	1
1.2 Research Objectives.....	5
1.3 Thesis Overview	6
CHAPTER 2 REVIEW OF LITERATURE	9
2.1 Tool Steels and Premium H13	9
2.2 Quenching Process and Martensite Transformation of Tool Steels	10
2.3 Kinetics for Martensite Transformation	12
2.4 Plastic Strain and Residual Stress	13
2.5 Models and Simulation of Heat Treatment.....	17
2.6 Major Challenges Facing the Modelling and Simulation of Heat Treatment and Quenching Process	23
2.7 Current Efforts to Standardize the Measurement of Steel Phase Transformation Kinetics and Dilatation Strains.....	26
2.8 Tensile Tests at Elevated Temperature	27
2.9 Gleeble Thermal –Mechanical Simulator and Resistance Heating	31
2.10 Other Methods of Heating.....	42
2.11 Summary	44

CHAPTER 3 FEA-AIDED DESIGN OF SPECIMEN	46
3.1 Experimental Materials	46
3.2 Design of the Specimen	47
3.3 Resistance Heating Simulation and Optimization for the Design of the Tensile Specimen	54
3.4 Optimizing the Specimen Geometry	62
3.4.2 The Influence of the Thickness of the Connecting Bridges	76
3.5 Tensile Simulation	82
CHAPTER 4 EXPERIMENTAL VERIFICATION OF DESIGN CONCEPT	87
4.1 Description of Tensile Test Chamber	87
4.2 Experiments on the Heating and Cooling Behaviour of Samples with Different Dimensions	90
4.3 Cooling Behaviour with or without Gas Cooling	110
4.4 Experiment to Study the Strength of the Connecting Bridges on the Tensile Test	114
CHAPTER 5 DISCUSSION AND CONCLUSIONS	119
5.1 Discussion and Conclusions	119
CHAPTER 6 CONTRIBUTIONS AND FUTURE WORK	124
6.1 Contributions	124
6.2 Future Work	125
APPENDICES	126
APPENDIX A: PHYSICAL PROPERTIES FOR BOHLER SUPERIOR (PREMIUM H13)	126
APPENDIX B: A PARAMETER STUDY PROGRAM TO INVESTIGATE THE STEADY-STATE TEMPERATURE DISTRIBUTION UNDER DIFFERENT APPLIED CURRENT DENSITY	127
APPENDIX C: POST-PROCESSING PROGRAM IN PYTHON TO ANALYZE THE TEMPERATURE DISTRIBUTION ALONG THE LENGTH OF THE SAMPLE	129
REFERENCES	131
VITA AUCTORIS	137

LIST OF FIGURES

FIGURE 2.1 DILATOMETER CURVE, TYPICAL VOLUME CHANGE OF A TRANSFORMED STEEL.....	11
FIGURE 2.2 DEVELOPMENT OF RESIDUAL STRESS DURING COOLING OF STEEL.....	14
FIGURE 2.3 COUPLING BETWEEN THERMAL, METALLURGICAL AND MECHANICAL INTERACTIONS.....	17
FIGURE 2.4 SIMULATION RESULTS OF RESIDUAL STRESS DISTRIBUTION IN A GEAR AFTER QUENCHING .	21
FIGURE 2.5 SIMULATION RESULT OF DEFORMATION OF A CRANKSHAFT AFTER QUENCHING .	21
FIGURE 2.6 CCT DIAGRAM FOR PREMIUM H13 FROM UDDELHOM	24
FIGURE 2.7 A SIMPLE TENSILE TEST SETUP	28
FIGURE 2.8 VACUUM CHAMBER IN GLEEBLE 1500 SIMULATOR.....	32
FIGURE 2.9 SCHEMATIC ILLUSTRATION OF RESISTANCE HEATING IN GLEEBLE MACHINE.....	33
FIGURE 2.10 STANDARD SAMPLE FOR GLEEBLE MACHINE	36
FIGURE 2.11 THE SIMULATED PROFILE OF TEMPERATURE DISTRIBUTION.....	36
FIGURE 2.12 STANDARD TENSILE SAMPLE WITH VARYING CIRCULAR CROSS SECTION	37
FIGURE 2.13 SIMULATION RESULT OF THE TEMPERATURE PROFILE	38
FIGURE 2.14 ANALYSIS OF ANOTHER SPECIFICALLY DESIGNED SAMPLE	39
FIGURE 2.15 SIMULATION RESULT OF TEMPERATURE PROFILE ALONG THE CENTRAL LINE OF THE SPECIAL SPECIMEN	40
FIGURE 2.16 THE END-HEATING ELEMENT FOR TORSION TESTING	42
FIGURE 2.17 THE INSTALLATION OF THE END-HEATING ELEMENT WITH.....	42
FIGURE 3.1 SPECIMEN FOR QUENCHING SIMULATION AND TENSILE TESTING	50
FIGURE 3.2 SEVEN SECTIONS OF THE SAMPLE.....	51
FIGURE 3.3 SCHEMATIC ILLUSTRATION OF CURRENT FLOW IN THE SAMPLE DURING RESISTANCE HEATING .	52
FIGURE 3.4 THE HALF OF THE SPECIMEN TO BE MODELLED	54
FIGURE 3.5 THERMAL CONDUCTIVITY VARIATION WITH TEMPERATURE FOR BOHLER W302 SUPERIOR /PREMIUM H13	58
FIGURE 3.6 ELECTRIC RESISTIVITY VS TEMPERATURE FOR BOHLER W302 SUPERIOR /PREMIUM H13.....	58

FIGURE 3.7 THE TEMPERATURE OF THE MIDDLE NODE IN THE GAUGE AREA CHANGES WITH THE END BOUNDARY ELECTRICAL CURRENT DENSITY FOR A SAMPLE WITH THE EXTENSION ZONES OF 30MM IN LENGTH AND CONNECTING BRIDGES OF 0.6MM IN THICKNESS.	66
FIGURE 3.8 SIMULATION RESULT OF THE TEMPERATURE PROFILE FOR A SAMPLE	70
FIGURE 3.9 SIMULATION RESULT OF THE TEMPERATURE PROFILE ALONG THE CENTRAL LINE FOR A SAMPLE WITH THE EXTENSION SECTIONS OF 10MM IN LENGTH.	70
FIGURE 3.10 SIMULATION RESULT OF THE TEMPERATURE PROFILE FOR A SAMPLE	71
FIGURE 3.11 SIMULATION RESULT OF THE TEMPERATURE PROFILE ALONG THE CENTRAL LINE FOR A SAMPLE WITH THE EXTENSION SECTIONS OF 20MM IN LENGTH.	71
FIGURE 3.12 SIMULATION RESULT OF THE TEMPERATURE PROFILE FOR A SAMPLE	72
FIGURE 3.13 SIMULATION RESULT OF THE TEMPERATURE PROFILE ALONG THE CENTRAL LINE FOR A SAMPLE WITH THE EXTENSION SECTIONS OF 30MM IN LENGTH.	72
FIGURE 3.14 SIMULATION RESULT OF THE TEMPERATURE PROFILE FOR A SAMPLE	73
FIGURE 3.15 SIMULATION RESULT OF THE TEMPERATURE PROFILE ALONG THE CENTRAL LINE FOR A SAMPLE WITH THE EXTENSION SECTIONS OF 40MM IN LENGTH.	73
FIGURE 3.16 SIMULATION RESULT OF THE TEMPERATURE PROFILE FOR A SAMPLE	74
FIGURE 3.17 SIMULATION RESULT OF THE TEMPERATURE PROFILE ALONG THE CENTRAL LINE FOR A SAMPLE WITH THE EXTENSION SECTIONS OF 50MM IN LENGTH.	74
FIGURE 3.18 SIMULATION RESULT OF THE TEMPERATURE PROFILE FOR A SAMPLE	77
FIGURE 3.19 SIMULATION RESULT OF THE TEMPERATURE PROFILE ALONG THE CENTRAL LINE FOR A SAMPLE WITH CONNECTING BRIDGES OF 0.45MM IN THICKNESS	77
FIGURE 3.20 SIMULATION RESULT OF THE TEMPERATURE PROFILE FOR A SAMPLE	78
FIGURE 3.21 SIMULATION RESULT OF THE TEMPERATURE PROFILE ALONG THE CENTRAL LINE FOR A SAMPLE WITH CONNECTING BRIDGES OF 0.30MM IN THICKNESS	78
FIGURE 3.22 SIMULATION RESULT OF THE TEMPERATURE PROFILE FOR A SAMPLE	80
FIGURE 3.23 SIMULATION RESULT OF THE TEMPERATURE PROFILE ALONG THE CENTRAL LINE FOR A SAMPLE WITH CONNECTING BRIDGES OF 0.75MM IN THICKNESS	80

FIGURE 3.24 THE SIMULATION RESULT OF THE TEMPERATURE PROFILE FOR A SAMPLE WITH EXTENSION ZONE LENGTH OF 30MM, BRIDGE THICKNESS OF 0.6MM WHEN THE MIDDLE OF THE GAUGE LENGTH IS COOLED TO 300°C.	84
FIGURE 3.25 THE SIMULATION RESULT OF THE PROFILE OF STRESS s_{11} FOR A SAMPLE WITH EXTENSION ZONE LENGTH OF 30MM, BRIDGE THICKNESS OF 0.6MM WHEN THE MIDDLE OF THE GAUGE LENGTH IS COOLED TO 300°C.	84
FIGURE 3.26 THE SIMULATION RESULT OF THE TEMPERATURE PROFILE FOR A SAMPLE WITH EXTENSION ZONE LENGTH OF 30MM, BRIDGE THICKNESS OF 0.75MM WHEN THE MIDDLE OF THE GAUGE LENGTH IS COOLED TO 300°C.	85
FIGURE 3.27 THE SIMULATION RESULT OF THE PROFILE OF STRESS s_{11} FOR A SAMPLE WITH EXTENSION ZONE LENGTH OF 30MM, BRIDGE THICKNESS OF 0.75MM WHEN THE MIDDLE OF THE GAUGE LENGTH IS COOLED TO 300°C.	86
FIGURE 4.1 VACUUM ELECTRIC RESISTANCE HEATING SYSTEM WITH WATER COOLING AND GAS QUENCHING	87
FIGURE 4.2 TEMPERATURE PROFILE FOR A SAMPLE WITH EXTENSION LENGTH OF 30MM AND CENTRAL ZONE WIDTH OF 40MM.....	91
FIGURE 4.3 HEATING AND COOLING CURVES OF SAMPLE A.....	91
FIGURE 4.4 TEMPERATURE DIFFERENCES REACHED DURING THE HEATING AND COOLING PROCESS FOR SAMPLE A.....	92
FIGURE 4.5 CONDUCTIVE HEAT FLOW IN SAMPLE A WHEN HEATED TO A PEAK TEMPERATURE OF 980°C...	93
FIGURE 4.6 TEMPERATURE PROFILE WITH TIME DURING THE RESISTANCE HEATING AND COOLING FOR SAMPLE D WITH THE MODIFIED FLANK WIDTH OF 10MM AND BRIDGE CONNECTORS THICKNESS OF 1MM.	94
FIGURE 4.7 TEMPERATURE VARIATION WITH TIME DURING THE RESISTANCE HEATING AND COOLING FOR SAMPLE D WITH THE MODIFIED WING WIDTH OF 10MM AND CONNECTOR THICKNESS OF 1MM.	95
FIGURE 4.8 TEMPERATURE DIFFERENCE DURING THE HEATING AND COOLING FOR SAMPLE D.....	96
FIGURE 4.9 TEMPERATURE PROFILE OF SAMPLE E WITH THE TRIMMED TRANSITIONAL AREAS WHEN HEATED TO 1020°C IN THE CENTRAL GAUGE AREA.	98

FIGURE 4.10 TEMPERATURE VARIATION DURING HEATING AND COOLING FOR SAMPLE E.....	98
FIGURE 4.11 TEMPERATURE DIFFERENCE DURING HEATING AND COOLING FOR SAMPLE E.....	99
FIGURE 4.12 TEMPERATURE PROFILE OF SAMPLE F WITH EXTENSION SECTION LENGTH OF 30MM EACH AND THE BRIDGE CONNECTORS 12MM WIDE AND 0.8MM THICK WHEN HEATING ABOVE 900°C.....	100
FIGURE 4.13 TEMPERATURE VARIATION DURING HEATING AND COOLING FOR SAMPLE F.....	101
FIGURE 4.14 TEMPERATURE DIFFERENCE FOR SAMPLE F.....	101
FIGURE 4.15 TEMPERATURE PROFILE OF SAMPLE H WITH EXTENSION SECTION LENGTH OF 30MM EACH AND THE CONNECTING BRIDGES 12MM WIDE AND 1.0MM THICK WHEN HEATING UP TO ABOUT 950°C.	104
FIGURE 4.16 TEMPERATURE PROFILE OF SAMPLE I WITH EXTENSION SECTION LENGTH OF 30MM EACH AND THE CONNECTING BRIDGES 12MM WIDE AND 0.8MM THICK WHEN HEATING UP TO ABOUT 950C.	104
FIGURE 4.17 TEMPERATURE VARIATION DURING HEATING AND COOLING FOR SAMPLE H.....	105
FIGURE 4.18 TEMPERATURE DIFFERENCE DURING HEATING AND COOLING FOR SAMPLE H.....	105
FIGURE 4.19 TEMPERATURE VARIATION DURING HEATING AND COOLING FOR SAMPLE I.....	106
FIGURE 4.20 TEMPERATURE DIFFERENCE DURING HEATING AND COOLING FOR SAMPLE I.....	106
FIGURE 4.21 TEMPERATURE PROFILE OF SAMPLE J WITH EXTENSION SECTION LENGTH OF 20MM EACH AND THE CONNECTING BRIDGES 12MM WIDE AND 1.0MM THICK WHEN HEATED UP TO ABOUT 940°C.....	108
FIGURE 4.22 TEMPERATURE VARIATION DURING HEATING AND COOLING FOR SAMPLE J.....	109
FIGURE 4.23 TEMPERATURE DIFFERENCE DURING HEATING AND COOLING FOR SAMPLE J.....	109
FIGURE 4.24 TEMPERATURE VARIATION DURING HEATING AND COOLING (WITH GAS COOLING).....	111
FIGURE 4.25 TEMPERATURE DIFFERENCE DURING THE HEATING AND COOLING (WITH GAS COOLING).....	111
FIGURE 4.26 TEMPERATURE VARIATION DURING HEATING AND COOLING FOR SAMPLE F (WITHOUT GAS COOLING).....	113
FIGURE 4.27 TEMPERATURE DIFFERENCE FOR SAMPLE F WITHOUT GAS COOLING.....	113
FIGURE 4.28 TEMPERATURE DROP AT THE MIDDLE OF GAUGE LENGTH DURING COOLING.....	114
FIGURE 4.29 LEFT: QUENCHED SAMPLE WITH THE CENTRAL GAUGE AREA CUT.....	115
FIGURE 4.30 TENSILE TEST SET-UP.....	115
FIGURE 4.31 TEMPERATURE VARIATION DURING HEATING AND COOLING FOR SAMPLE G.....	117
FIGURE 4.32 TEMPERATURE DIFFERENCE DURING HEATING AND COOLING.....	117

LIST OF TABLES

TABLE 3.1 CHEMICAL COMPOSITION OF BOHLER PREMIUM H13	46
TABLE 3.2 RADIATION EMITTANCE FOR STEEL	59
TABLE 3.3 PROPERTIES OF COPPER AND COPPER-NICKEL ALLOYS	60
TABLE 3.4 RADIATION EMITTANCE FOR NICKEL AND COPPER.....	621
TABLE 3.5 SIMULATION RESULTS OF THE TEMPERATURE OF THE MIDDLE NODE OF THE SAMPLE	65
TABLE 3.6 TEMPERATURES OF THE MIDDLE NODE OF THE SAMPLES FOR DIFFERENT SURFACE ELECTRICAL CURRENT DENSITY WHEN USING CONNECTING BRIDGES OF 0.45MM IN THICKNESS.....	67
TABLE 3.7 THE MAGNITUDE OF SURFACE ELECTRICAL CURRENT DENSITY APPLIED AT THE TWO ENDS REQUIRED TO HEAT THE SAMPLE'S MIDDLE NODE TO 1200°C.....	68
TABLE 3.8 THE INFLUENCE OF THE LENGTH OF EXTENSION ZONE.....	75
TABLE 3.9 THE INFLUENCE OF THE THICKNESS OF CONNECTING BRIDGES	81
TABLE 4.1 DIMENSIONS OF SAMPLE A.....	90
TABLE 4.2 DIMENSIONS OF THE SAMPLE D.....	94
TABLE 4.3 DIMENSIONS OF THE SAMPLE E	97
TABLE 4.4 DIMENSIONS OF THE SAMPLE F	100
TABLE 4.5 DIMENSIONS FOR SAMPLE H AND I:.....	103
TABLE 4.6 DIMENSIONS FOR SAMPLE J.....	108
TABLE 5.1 SUMMERY OF EXPERIMENTAL DATA.....	122

CHAPTER 1 INTRODUCTION

1.1 Motivation

Heat treatment is an indispensable industrial process to modify properties of steels to suit particular applications. As one kind of heat treatment process, quenching has been known for thousands of years to be the most effective process to harden steels, and it is used extensively throughout the industry to produce high strength steels.

Although the strengthening mechanisms of quenching, and the phase transformation during the heat treatment process, have been the subjects of research over a century, the complicated coupling of thermal, phase transformation and stress/strain changes make the description of heat treatment process more qualitative than quantitative. Thermal and residual stresses develop during heat treatment and quenching, and can result in distortion and even cracking. The latter leads to time consuming and expensive corrective measures of rework and repair welding. Residual stresses can reduce the service performance of steel and result in catastrophic failure during service. Because of the lack of ability to precisely predict the potential level of residual stress, distortion and/or cracking during and after quenching, the design of a heat treatment process generally depends on experience, and may involve a tedious trial and error process. Aggressive quenching is usually avoided so the strengthening ability of quenching cannot be used at its extreme limit, so the depth of effective quench and the improvement in properties are usually compromised.

Over the last three decades, different models have been presented to describe the martensite microstructure evolution and its influence on the mechanical properties and behaviour of steels during the process of quenching. Those developments have led both to atomic level and to finite element simulations to predict the residual stress, deformation and even fracture during quenching process. There are a variety of FEA-based software packages such as SYSWELDTM [1], DEFORMTM -HT[2], and DANTETM [3], which have been developed and commercialized to predict distortions and stresses resulting from heat treatment. These packages have been quite successfully used to conduct heat treatment simulation, to predict the residual stress and distortion brought about by a prescribed heat treatment process[4] and to do process optimization.

Despite these different approaches to the simulation of the quenching process, one thing remains the most difficult and challenging. How to measure the transient mechanical properties of the steel at the elevated temperatures during the quenching process when the microstructure of steel is a mixture of martensite and austenite? These transient temperature and microstructure - dependent mechanical properties of steels at elevated temperatures during quenching process are very difficult to measure experimentally due to the fact that the temperature of steels decreases dramatically from a high austenite temperature to a low temperature, usually room temperature in a very short time. During this time there are microstructure transformations, which include significant volume change and rapid and very large changes in strength and ductility.

Therefore, the mechanical properties of these partially transformed steels are usually not available in literature. But they are crucial for conducting a credible simulation to predict the residual stress, deformation and cracking phenomena during a quenching process. Without those data, it is impossible to predict the onset of quench cracking during and after quenching.

Some of the temperature-dependent mechanical properties that do exist in the literature are achieved by heating the already quenched steel samples to the desired temperature and conducting the tensile test. These data can be seen only as the properties of fully quenched martensite (with minimal tempering for high alloy steels) at only slightly elevated temperature. They do not give the properties of the austenite-martensite mixtures which would exist at these elevated temperatures during quenching. The mechanical properties suitable for use in the simulation of quenching process should be achieved by conducting in-situ tensile test during the quenching process where the microstructure of steel is the mixture of new martensite and the retained austenite which exists at that temperature.

Nowadays, for FEA simulations, the most-practiced method to deal with the data used for austenite-martensite microstructures in the simulation of quenching process is by using the rule of mixtures. Since the microstructure of steel during quenching is a mixture of martensite and austenite, the mechanical properties for the mixed phase is usually derived by applying this rule to the properties of martensite and austenite.

However, the correctness of the derived properties highly depends on the precision of elevated temperature mechanical properties of martensite and austenite, which are also difficult to measure and obtain. And for the complicated microstructure of mixed martensite and austenite, the properties cannot be derived simply by using a linear mixing rule. Since the austenite is a soft phase, it is obvious that it will yield first when subjected to a stress lower than the gross yield stress derived by using the rule of mixtures. Moreover, the ductility of the mixtures cannot be predicted from this rule of mixtures.

In recent years, many sophisticated testing machines like the Gleeble1500/3500 have been developed to conduct dynamic thermal-mechanical tests. These machines rely on resistance heating or induction heating to heat the samples. Because both ends of the sample are gripped and cooled, the middle cross-section of the sample always has the highest temperature. Due to these characteristics, the Gleeble machines are particularly suitable for conducting welding and joining tests. For mechanical property tests, because it is hard to achieve a uniform temperature distribution along the gauge length of samples, few tensile tests have been reported. Much more of the reported results are for compression testing, with the measurement of the strain calculated from the diameter change of the middle cross-section diameter. Because the compression results cannot predict tensile failure, and tensile tests can give out much more useful mechanical data such as fracture strain, data from tensile tests are much more desirable than those from compression tests.

A special kind of tensile specimen is needed, which can utilize the convenience of resistance heating, as in the Gleeble machine, and which can maintain a uniform temperature distribution along its gauge length at elevated temperatures during quenching. The maintenance of a uniform temperature is difficult to obtain, but is necessary to properly measure the mechanical properties at elevated temperatures during the quenching process.

1.2 Research Objectives

The main objective of this research is to develop a tensile test method that will be capable of measuring the transient mechanical properties of the steel at the elevated temperatures experienced throughout the quenching process.

The methods include:

- Design a special kind of tensile specimen to be used in a resistance heating device, which will have a sufficiently uniform temperature distribution along the gauge length of the sample. This uniform temperature will be achieved at any of the different temperatures present when the specimen goes through the entire heating and cooling process encountered during quenching. The temperature of the specimen should be able to be controlled conveniently during quenching, so the tensile test can be successfully conducted at a specified testing temperature. This includes the case when the specimen has been directly quenched to a preset temperature, and is held there for testing. The specimen must be able to change

temperatures rapidly, and quickly establish the uniform temperature without significant overshoot.

- Conduct FEA-based resistance heating and tensile simulations for different dimensions of the specimen to study the influence of dimension changes on the temperature distribution of the specimen, and its suitability for use in tensile tests.
- Validate the feasibility of this design concept through experiments. The temperature distribution along the length of the sample will be measured to determine the optimum dimensions of the sample for the purpose of achieving a uniform temperature distribution.

1.3 Thesis Overview

Chapter 2 first introduces the tool steel H13, which is the material of our research interest, its quenching process and phase transformations. Theories for the kinetics of martensite transformation, plastic strain and residual stress, and different approaches of modeling and simulation of heat treatment are then reviewed.

It is pointed out that the main challenge facing the simulation of heat treatment and quenching process is the lack of the essential mechanical properties at elevated temperatures during quenching process. The ASTM standards have been reviewed, only to find that there is no standardized method suitable for the tensile test at elevated temperatures for steels during quenching process.

Resistance heating is an effective method to heat steels, as it has been implemented in Gleeble machines. Different types of specimens, proposed by other authors, have been reviewed and analyzed through resistance heating simulation. These specimens have either the problem of being hard to achieve a uniform temperature distribution along the gauge length or the problem of being unsuitable for tensile testing. It becomes obvious that another kind of specimen must be designed to overcome the disadvantages of those samples. This new specimen must be able to quickly achieve a uniform temperature distribution along the gauge length at different elevated temperatures, and must also be suitable for in-situ tensile tests during quenching process.

Chapter 3 describes the concept of how to design a special kind of specimen for our specific material, H13, in order to conduct tensile tests successfully in the physical simulation of the quenching process. Resistance heating simulations have been conducted to do parametric studies for the dimensions of the sample in order to find the optimized dimensions for achieving a uniform temperature distribution along the gauge length of the sample. Also the design concept is also pre-verified to be mechanically sound through the stress simulation of the sample under tensile load.

Chapter 4 first describes the design and construction of a steel vacuum chamber used for the resistance heating of the specifically designed sample. The observation of the temperature distributions found for the sample will be compared with the predictions from the FEA simulation. The evolution of the modification of the design of the sample

will be made according to the previous experimental results and the new results will be further verified through experiment.

Chapter 5 will give out the conclusions of this approach to design and validate the feasibility of the specially-designed specimen to conduct the physical simulation of quenching. Its suitability for doing in-situ tensile tests to obtain mechanical properties at elevated temperature for different stages in the quenching process will be discussed.

CHAPTER 2 REVIEW OF LITERATURE

2.1 Tool Steels and Premium H13

Tool steels belong to an extension of alloy steels, specifically designed and manufactured under critical control to meet special quality requirements. In general, because they are used to cut or form other steels, they often are used at very high hardness levels. They usually contain significantly more alloying elements than other alloy steels [5].

The significant increase of alloying elements in tool steels enhances their hardenability greatly, and permits quenching conditions which are less severe to obtain a fully hardened martensite microstructure, especially in thick sections, or sections with a complex geometry. The existence of predominant martensite in fully hardened tool steels is the most significant microstructure feature which differentiates them from general steels.

Among all tool steels, premium H13 is one of the most popular and available hot work tool steels. It is a chromium hot-work tool steel and is used throughout industry for general hot-work applications: 1) light metal die casting dies; 2) metal extrusion dies; 3) hot forging dies; 4) plastic mould cavities. Because it will often be subjected to both high cyclic thermal stresses, and in some cases impact loading, the carbon levels are lower than most tool steels. Lowering the carbon level improves fracture toughness. Increasing the fracture toughness in this case means increasing the resistance to both the initiation

and the propagation of cracks. The typical composition (Wt. %) of H13 is 0.35C 1.5Mo 5.0Cr and 1.0V. The addition of refractory metals such as W, Mo, Cr and V tends to form carbides on tempering that inhibit dislocation motion and reduce the softening effects of heat. Most importantly, they produce secondary hardening, which is an increase in hardness on tempering. The family of chromium hot-work tool steel (H10 to H19) types resist softening at temperatures up to 430°C.

In this research, the Premium H13 grade steel donated by BOHLER UDDEHOLM LIMITED has been chosen as the steel to be studied.

2.2 Quenching Process and Martensite Transformation of Tool Steels

A typical hardening process for hot work tool steel is comprised of two stages: austenitising and quenching. During the austenitising stage, the tool steel work piece is heated in a protective atmosphere to its austenitising temperature, and is held at that temperature for a time long enough to ensure the total dissolution of carbide and alloy elements in the austenite. For large pieces, usually a two-stage heating is scheduled to ensure uniform heating up to over 1000°C. During the quenching stage, the work piece is cooled quickly enough to form martensite, generally using forced convective cooling with nitrogen gas. Rapid cooling from over 1000°C to about 500°C is very important, because this will suppress the precipitation of grain boundary non-ferrous carbides, as well as the formation of soft phases like bainite, ferrite and pearlite. The objective is to obtain martensite as the only predominant phase.

The martensite transformation from austenite is a diffusionless phase transformation. The closely-packed FCC structure of austenite is transformed to a less densely packed body-centered tetragonal (BCT) structure of martensite. Figure 2.1 shows the typical volume change of a transformed steel in the form of a dilatometer plot. The heating curve shows the change of the room temperature ferrite and carbide microstructure to the single phase austenite, which has close-packed atomic structure and therefore shrinkage occurs. On quenching, the austenite cools to a temperature well below the temperature at which it is stable and transforms to a BCT structure of martensite. Accompanying this quenching process, there is a volumetric expansion. This metallurgical transformation expansion contributes to deformation, distortion, and residual stresses, and can even cause cracking.

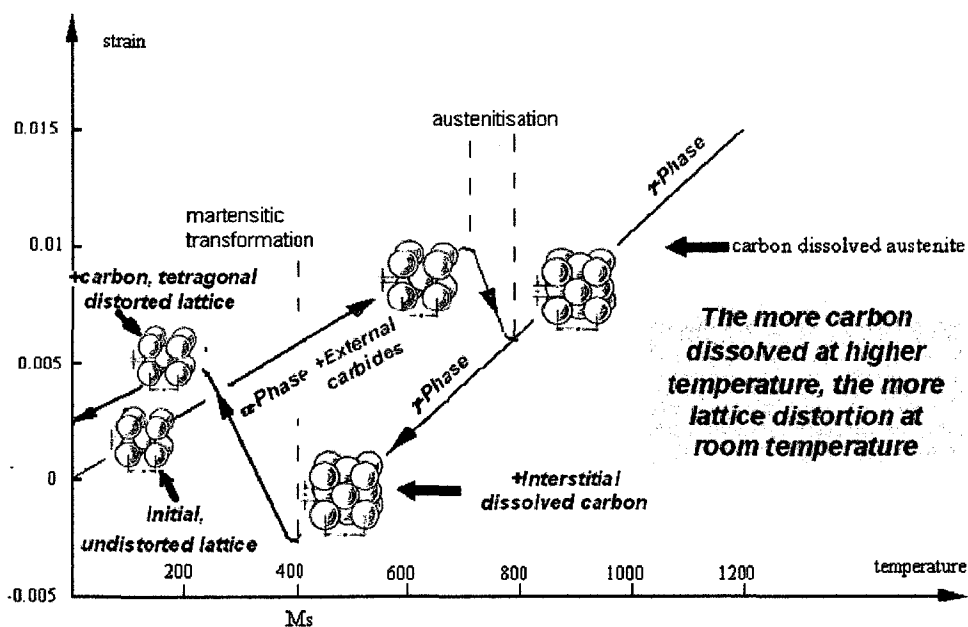


Figure 2.1 Dilatometer curve, typical volume change of a transformed steel[6]

2.3 Kinetics for Martensite Transformation

During the quenching process, the austenite to martensite reaction in steel is considered to be a time independent (athermal) diffusionless shear process. Below the martensite start temperature, M_s , martensite transformation is independent of time and depends only on the temperature at which it occurs. The reaction is essentially instantaneous, and the volume fraction of martensite formed is that which represents the lowest Gibb's Free Energy for the coexistence of austenite and martensite. The volume percentage of martensite transformed from austenite $\xi(T)$ at a given temperature of T can be estimated by the semi-empirical relation developed by Koistinen-Marburger [7]

$$\xi(T) = 1 - \exp[-b(M_s - T)] \quad (1)$$

where b was found to be close to $0.011K^{-1}$.

At the martensite finish temperature, M_f , all the austenite will become martensite. For tool steels, M_f is well below $0^\circ C$. Some authors [8,9,10] have used the following equation to calculate the martensite fraction $\xi(T)$ transformed from austenite.

$$\xi(T) = 1 - \left(\frac{T - M_f}{M_s - M_f} \right)^p \quad (2)$$

where p is assumed to be 2 or 2.5 [8,10].

The effect of stress on the martensite transformation starting temperature, M_s , has also been studied and observed. Tensile stress will increase M_s while compression will lower it. A modified Koistinen-Marburger equation incorporating a stress factor σ_m can be expressed as the following equation.

$$\xi(T) = 1 - \exp[-b(M_s - T) - \psi(\sigma_m)] \quad (3)$$

where $\psi(\sigma_m)$ is a function of stress component.

2.4 Plastic Strain and Residual Stress

Residual stress and deformation result from the non-uniform temperature distribution during the quenching process. As shown in Figure 2.2, H. W. Walton et al [11] have given a good illustration of residual stress development during quenching process.

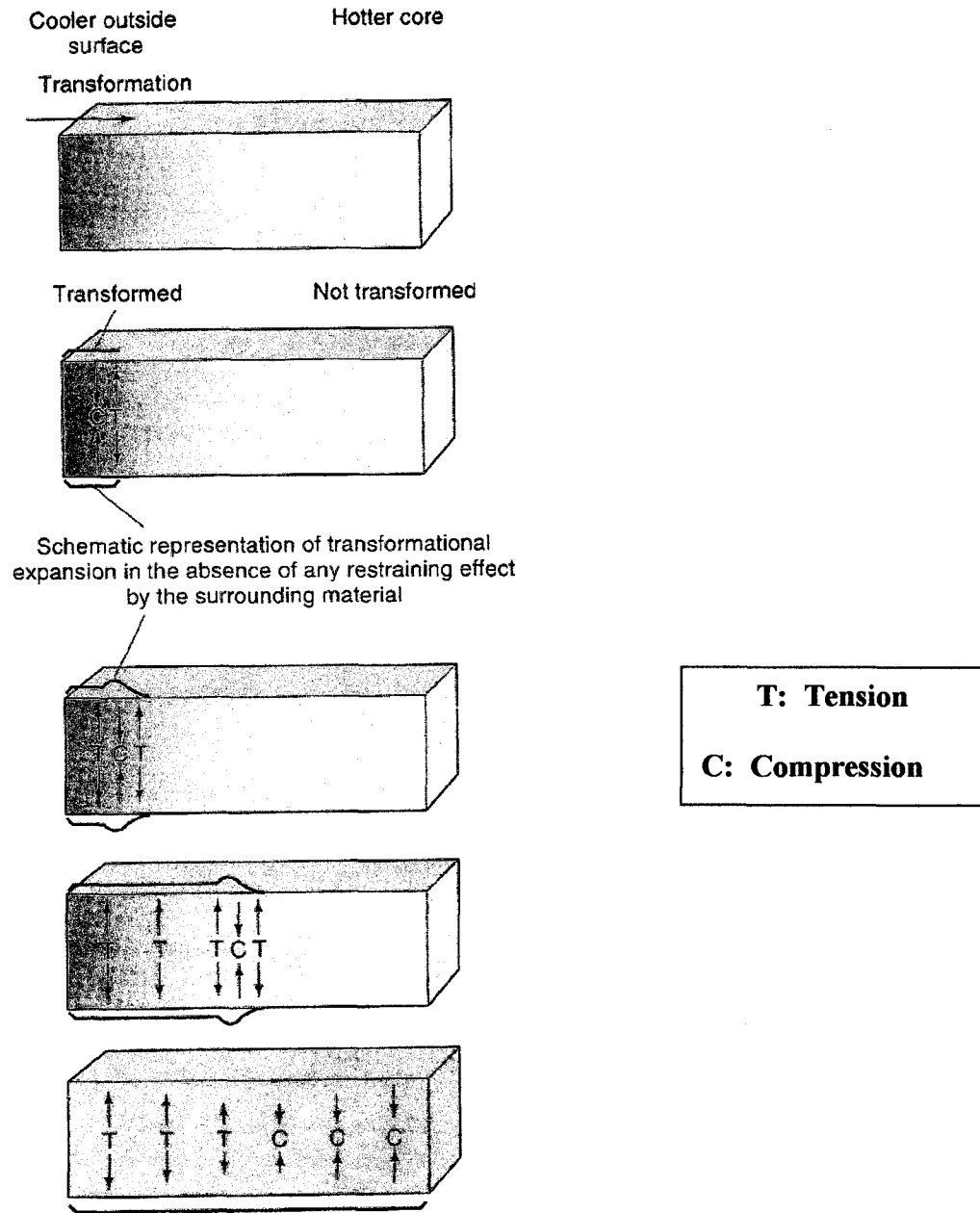


Figure 2.2 Development of residual stress during cooling of steel [11]. The brick shape represents a mathematical element from a block of steel bigger than this page. The left-hand side of the element is at the surface being quenched. The rest of the element extends into the interior. It shows how the residual stresses change as the transformation interface moves into the bulk of the materials.

Cooling and the martensite transformation happen first on the surface and then extend toward the core of steel block as the interior cools by conduction. Because of the volume expansion when austenite transforms to martensite, the first transformed martensite will be subject to the compressive restraint by the austenite matrix while that matrix will be stretched in tension to maintain continuity, and to obey force equilibrium on a free body section.

While it is still at high temperatures, the austenite matrix will be able to yield easily to accommodate the surface martensite, and so can relax the compression in the first formed martensite. As the transformation goes deeper into the body of the part, the expansion of the newly formed martensite will further put the austenite in front of it in tension, and also act to stretch the previously formed martensite. The result will be that if the surface martensite had any remnant compressive stress, then this will be further relaxed. If it had already reached the relaxed state, then it will develop tensile stresses.

It is important to remember that during quenching, the temperature in the remaining core of austenite will cool from about 1030°C to the M_s temperature, which is about 320°C, and then will form austenite-martensite mixtures down to room temperature. As the temperature of the non-transformed austenite becomes cooler, its yield strength increases, and it becomes less able to relax the stresses caused by the encroaching transformation front.

So in summary, when there is a thin skin of transformation product at the surface, then the still very hot austenite core can yield so as to relax the misfit strains, leaving the martensite skin relatively stress free. As the interior austenite grows cooler and stronger, its ability to allow the newly transformed martensite to relax becomes less effective. When the final core of austenite transforms, it expands and there is minimal ability of the previously transformed product to relax. So the transformation of the final core causes stretching everywhere, and this is most severe in the previously completely relaxed skin.

The details of the final stress distribution are strongly affected by the relative strength of the austenite throughout the process. To model this correctly, it is important to know the mechanical properties of the austenite and the austenite-martensite mixtures from 1030°C all the way down to room temperature. It is the measurement of these properties that the new tensile specimen described in this thesis has been designed to accomplish.

At room temperature, about twenty percent of the steel at that temperature will be retained untransformed austenite, regardless of whether it is at the surface or deep in the interior of the body.

The relative amount of austenite transformed to martensite at any temperature can be inferred from the overall changes in volume of the bulk materials, or it can be measured directly by neutron or X-ray diffraction. But the mechanical properties of these mixtures have proven to be difficult to measure, except at temperatures close to ambient. The final residual stress will demonstrate a profile of surface in tension and the core in

compression. It is this tensile stress on the surface which causes the cracking of steel during quenching.

2.5 Models and Simulation of Heat Treatment

The phenomenon of the heat treatment process is quite complicated and involves the coupling of thermal, metallurgical and mechanical interactions as shown in Figure 2.3.

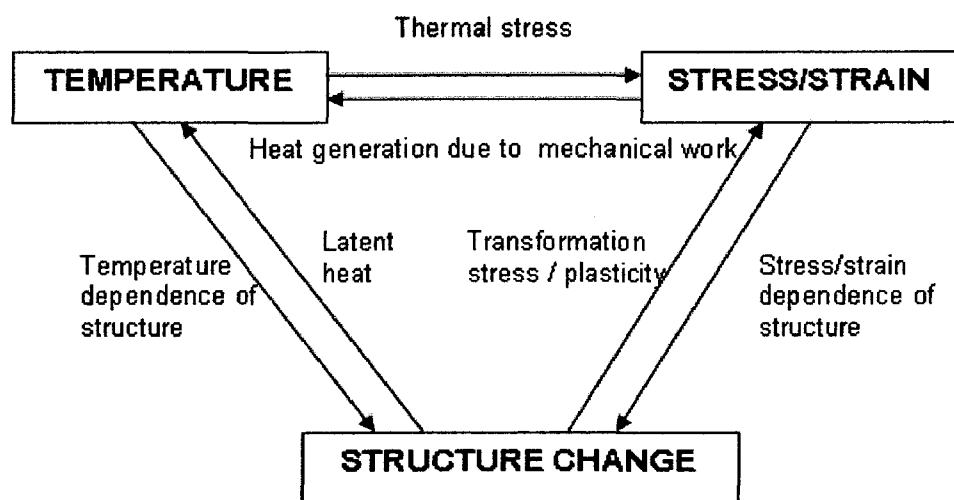


Figure 2.3 Coupling between thermal, metallurgical and mechanical interactions[12]

Temperature distribution changes in steel may cause temperature dependent phase transformations and thereby change its microstructure. For the quenching process, the Koistinen-Marburger equation mentioned above is usually applied to estimate the volume percent of martensite and austenite. Independent of the metallurgical changes, non-uniform temperature changes will cause thermal stress in the steel.

The microstructure change will bring about latent heat related thermal effects and change the temperature distribution. Also the microstructure change will be accompanied by transformation strain and plasticity. Transformation plasticity is associated with two physical phenomena. One is called the Greenwood-Johnson mechanism [13]: the volume variations between the phases generate microscopic internal stresses which are sufficient to induce plastic strain in the weaker phase, e.g. martensite deforming austenite. The second is called the Magee mechanism: anisotropic orientation of the transformed phase due to applied stress, which only exists for the martensite transformation. In the presence of an external stress, martensite needles are formed in a preferential direction.

For different models of transformation-induced plasticity, the transformation-induced plasticity is proposed as follows:

- $\varepsilon^{tp} = \frac{5}{6\sigma_y^y} \frac{\Delta V}{V} \sigma$ Greenwood and Johnson model[13]
- $\varepsilon^{tp} = \frac{1}{4\sigma_y^y} \frac{\Delta V}{V} (3p - 2p^{3/2})\sigma$ Abrassart model[14]
- $\varepsilon^{tp} = \frac{2}{3\sigma_y^y} \frac{\Delta V}{V} (p \log p - p)\sigma$ Leblond model[15]

Where $\frac{\Delta V}{V}$ represents the relative volume variation between the phases during transformation and σ_y^y the yield stress of austenite.

Stress/strain evolution will induce phase transformations and changes in the microstructure as is shown in the modified Koistinen-Marburger equation, which models the effect of stress on the martensite transformation starting temperature. The mechanical work of deformation will be partially turned into heat and this will further change the temperature distribution.

Many authors have tried to incorporate all the coupled phenomena between thermal, metallurgical and mechanical interactions in heat treatment to create different models to calculate thermal history, phase transformation and stress/strain evolution. They then apply these models to predict residual stress and deformation in heat treatment.

T. Inoue et al [12] created the metallo-thermo-mechanics model which couples stress-strain, thermal and metallurgical behaviour during the heat treatment process. The schematic description of this can be seen in Figure 2.3. This model has been implemented in the heat treatment FEA software “HEARTS” (HEAt tReaTment Simulation program) [16].

S. Denis, P. Archambault and E. Gautier et al [17] presented models for stress-phase transformation couplings in metallic alloys. Their work has been implemented in commercial heat treatment simulation software SYSWELD[18,19] and FORGE.

F. D. Fischer et al[20] has developed another model of elastoplasticity coupled with phase changes to describe materials experiencing phase transformation, in which he

introduced the term of transformation-induced plasticity (TRIP) as an additional strain rate term to the “classic” plastic strain rate term. This model can be properly implemented by using a user-supplied materials subroutine in ABAQUS.

Another important model describing the plastic behaviour of solids during solid-solid transformations for steels is presented by Jean-Baptiste Leblond et al [21]. It simply exploits the usual thermo-mechanical characteristics of materials, and assumes that the transformation plasticity phenomenon arises solely from the microscopic mechanism proposed by Greenwood and Johnson [13].

One of the most important and highly useful models of phase transformation in steel is presented by Lusk and his co-workers. Incorporating the phase transformation model of Lusk et al. [22,23,24,25] and the Bamman-Chiesa-Johnson (BCJ) materials model [11,26,27,28], the DANTE heat treatment simulation software has been developed to predict heat treatment distortions and residual stresses during steel heat treatment. Some simulation results are shown in Figure 2.4 and Figure 2.5.

DANTETM can be provided as a set of user subroutines for ABAQUS finite element solvers. The simulation results from this software are claimed to agree with measurement in a relative sense (within about 15%) regarding microstructure, deformation and residual stress. There are many examples of its application for the prediction of part distortions both during and after heat treatment. It does not claim to be able to predict local cracking probability.

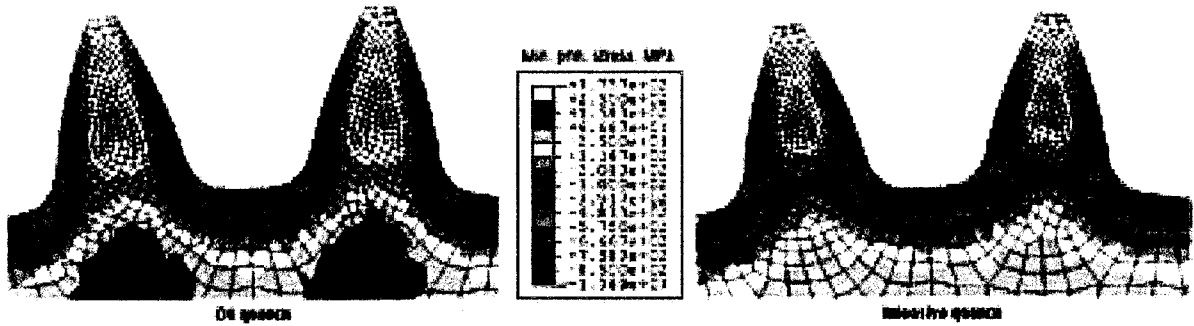


Figure 2.4 Simulation results of residual stress distribution in a gear after quenching [4].

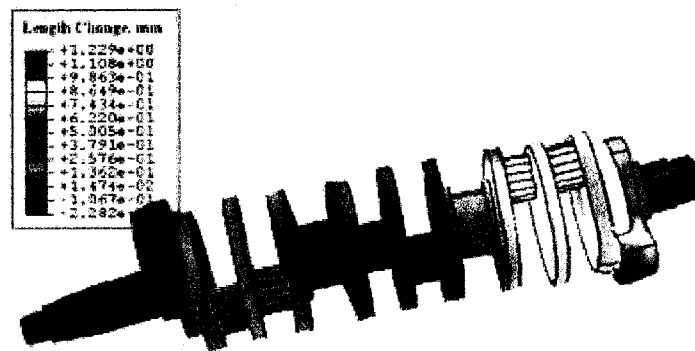


Figure 2.5 Simulation result of deformation of a crankshaft after quenching [4].

Generally, the following equation governing energy conservation takes into consideration of heat transfer, plastic work and latent heat:

$$\rho C_p \frac{\partial T}{\partial t} - \text{div}(k \text{grad} T) - \sigma_{ij} \dot{\epsilon}_{ij}^p + \sum \rho_j l_j \dot{\xi}_j = 0 \quad (4)$$

where :

ρ is mass density.

C_p is specific heat

k is heat conductivity

T is temperature

t is time

σ_{ij} is stress tensor

$\dot{\varepsilon}_{ij}^p$ is plastic strain rate tensor

ρ_J is the mass density for the J th phase constituent.

l_J is the enthalpy for the J th phase constituent.

$\dot{\xi}_J$ is the change rate of the volume fraction for the J th phase constituent.

$\sigma_{ij} \dot{\varepsilon}_{ij}^p$ accounts for the plastic work and $\sum \rho_J l_J \dot{\xi}_J$ accounts for the latent heat resulting from phase transformations.

For the calculation of the stress and strain evolution under complex conditions of heat treatment, the key resultant parameter relies on how to determine the strain rate tensor $\dot{\varepsilon}_{ij}$. The total strain rate tensor is comprised of five components and has been expressed

as:

$$\dot{\varepsilon}_{ij} = \dot{\varepsilon}_{ij}^e + \dot{\varepsilon}_{ij}^{th} + \dot{\varepsilon}_{ij}^{tr} + \dot{\varepsilon}_{ij}^{tp} + \dot{\varepsilon}_{ij}^{in} \quad (5)$$

where:

$\dot{\varepsilon}_{ij}^e$ is the elastic strain rate.

$\dot{\varepsilon}_{ij}^{th}$ is the thermal strain rate

$\dot{\varepsilon}_{ij}^{tr}$ is the strain rate due to volume change associated with different phase transformations

$\dot{\varepsilon}_{ij}^{tp}$ is the transformation-induced plastic strain rate .

$\dot{\varepsilon}_{ij}^{in}$ is the inelastic strain rate.

Different models to simulate the heat treatment process mostly concentrate on how to calculate those strain rate elements.

2.6 Major Challenges Facing the Modelling and Simulation of Heat Treatment and Quenching Process

A major limitation of all modeling methods is the scarcity of accurate data, and this was true initially for heat treat simulation. The property data required is similar for any commercially available software package even though the way the data is used is unique and usually proprietary to each.

In order to determine the phase transformation parameters, continuous cooling transformation (CCT) diagrams as shown in Figure 2.6, isothermal transformation (TTT) diagrams, or raw data generated using ASTM standard A-1033 are the ways available to represent the phase transformation kinetics.

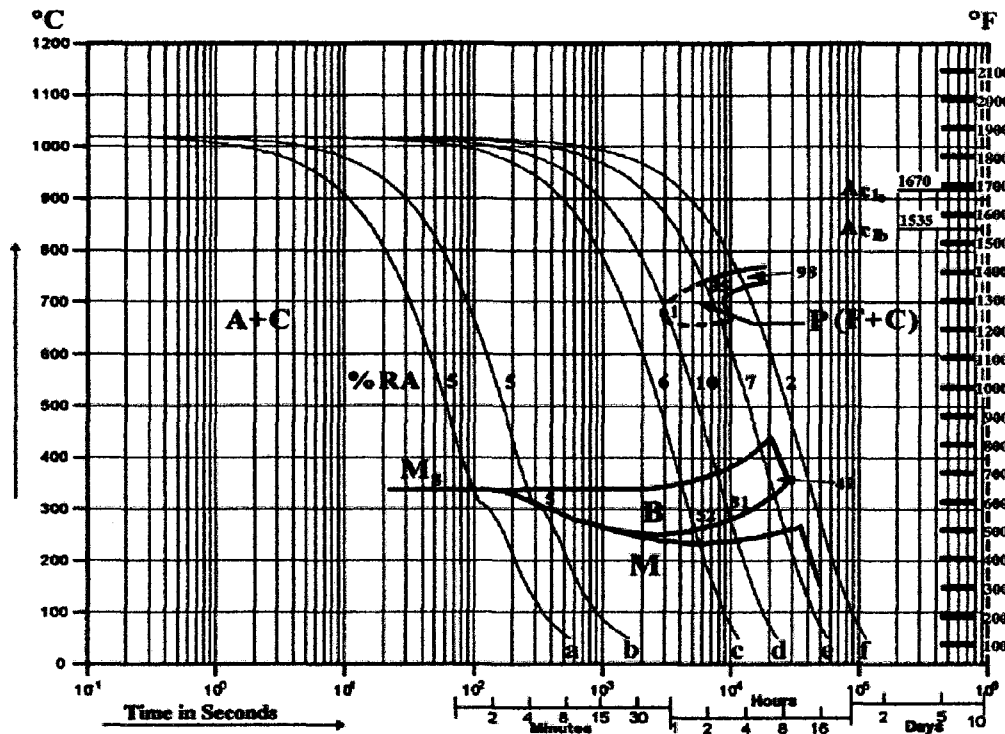


Figure 2.6 CCT Diagram for Premium H13 from Uddelhom[29]

A dilatometer can be used to measure the combined thermal strain and the strain due to volume change associated with phase transformation while steel goes through heat treatment.

But to determine transient mechanical properties of steels at elevated temperatures during heat treatment, especially during the quenching process remains a challenge. Experimental values for the tensile strength and yield stress for martensite, austenite, and their mixture at elevated temperature during quenching is critical to establish yield criteria, determine the transformation induced plasticity and predict the residual stresses, distortion and perhaps even fracture for all the models for heat treatment simulation.

In current practice of heat treatment simulation, the mechanical and physical properties χ of the steel are assumed to be expressed by the rule of mixtures as a linear combination of the properties χ_i of its constituents [30], such as pearlite, austenite, bainite, martensite, as shown in the following equation:

$$\chi = \sum_{J=1}^N \chi_J \xi_J \quad (6)$$

where $\sum_{J=1}^N \xi_J = 1$ and ξ_J denotes the volume fraction of the J th constituent .

As for quenched steel, its microstructure is a mixture of residual austenite and martensite. Since martensite is the hard phase embedded in the soft matrix of austenite, micro-yielding in austenite will occur when the stress is less than the yield stress derived from the rule of mixtures. To derive the mechanical properties of such a mixed microstructure, a non-linear rule of mixtures is used as given by Leblond[31]. The non-linear rule of mixtures for the yield stress of the mixture of martensite(hard) and austenite(soft) is expressed as the equation:

$$\sigma_y(T) = [1 - f(\xi_\alpha)]\sigma_y^\gamma(T) + f(\xi_\alpha)\sigma_y^\alpha(T) \quad (7)$$

Where:

$f(\xi_\alpha)$ is the non-linear function of the volume fraction of martensite ξ_α ;

$\sigma_y^\gamma(T)$ is the temperature-dependent yield stress of austenite;

$\sigma_y^\alpha(T)$ is the temperature-dependent yield stress of martensite.

This approach to calculate mechanical properties is only an approximation of the real world. They are based on the properties of single phases at different temperatures from the austenitizing temperature to room temperature, which are also quite difficult to obtain experimentally.

The precise mechanical data for austenite, martensite and mixtures of them during the quenching process can be obtained only through mechanical tests such as tensile or compression test at the transient temperature and state during the quenching process.

2.7 Current Efforts to Standardize the Measurement of Steel Phase Transformation Kinetics and Dilatation Strains

Currently, there are no open-literature reference sources or databases, providing both the kinetic and thermal strain components associated with steel phase transformations, for heat treatment process modeling and simulation. Data had been collected using non-standardised techniques, resulting in a wide variety of data that has not always proven to be useful for process optimisation in manufacturing operations. Standardized methods of measurement and data interpretation, necessary as a basis for the establishment of a quantitative database for process modeling, need to be developed. Accurate data will enable reliable predictive computer modeling of structures and residual stresses.

In 2001, a collaborative project sponsored by the US Department of Energy under AISI's Technology Roadmap Project on quantitative measurement of steel phase transformation (QMST) by the American Iron and Steel Institute (AISI) in co-operation with over a

dozen companies was launched [32]. The purpose of the QMST collaborative project was to develop a standard practice for obtaining and archiving quantitative steel transformation kinetics and thermal strain data. It has resulted in a new ASTM standard, A1033, "Practice for quantitative measurement and reporting of hypo-eutectoid carbon and low-alloys steel phase transformations"[33]. In this practice, the determination of hypo-eutectoid steel phase transformation behaviour by using high-speed dilatometry techniques for measuring linear dimensional change as a function of time and temperature has been defined.

But how to quantify transformation of austenite while a static elastic stress is applied to the austenite as well as transformation of the austenite while it is undergoing plastic deformation is highly challenging and remains as the future work for the QMST project.

2.8 Tensile Tests at Elevated Temperature

The standard test methods for elevated temperature tension tests of metallic materials has been specified in ASTM designation: E21-05 [34]. The tensile strength, yield strength, elongation and reduction of area of metallic materials at elevated temperatures can be determined from the tensile stress-strain curves. Those properties thereby obtained will be utilized in the estimation of the ability of materials to withstand the application of applied tensile forces under a variety of service conditions.

In the details of ASTM E21-05, Section 1.3 says that these test methods do not apply to rapid heating. Section 5.2.2, which lays out the allowable heating methods, says: “Heating shall be by electric resistance or radiation furnace with the specimen in air atmospheric temperature unless other media are specifically agreed upon in advance”. Throughout the rest of E21-05, it is clear that the document really assumes that the heating method is to enclose the specimen in a radiant furnace.

Figure 2.7 illustrates the simplest setup of a tensile test. Usually for tensile test at elevated temperatures, an electrical resistance or radiation furnace is built to provide heating and temperature maintenance for the tensile sample.

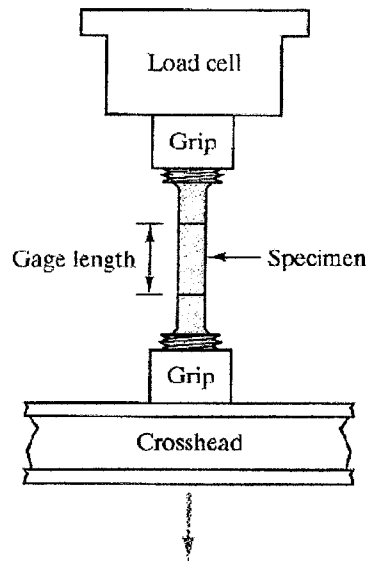


Figure 2.7 A simple tensile test setup [35]

The simplified description of an ordinary tensile specimen is that it typically comprises a long cylinder, the middle third of which length (the gauge section) has a circular cross-section whose diameter is about 0.5 to 0.7 that of the two end sections(the shoulders).

The tensile sample is gripped on the shoulders and pulled to measure its resistance to stretching forces. Reducing the diameter of the middle cross-section makes the stretching load per atom in the shoulders 0.25 to 0.49 times less than the load borne by atoms in the gauge section, so almost all the stretching occurs in the highly stressed gauge section.

For an above-mentioned ordinary tensile sample, the shoulders of the sample will heat up much more slowly than the gauge length and during rapid temperature changes, the middle and the end of the gauge length are at different temperatures. So the methods specified in ASTM E21-05 do not apply to rapid heating.

Also for both heating methods, the grips generally must be cooled, and so the grips cool the specimen shoulders, and the shoulders, unless they are very long, will cool the ends of the gauge length. This creates a significant temperature difference from the middle point of the gauge length to the ends of the gauge length. Experience using the Gleeble machine shows that even when using heated stainless steel grips the best temperature difference along the gauge length is about 60°C [36]. This is unacceptable according to ASTM E21 for elevated temperature tension tests of metallic materials.

In the quenching process, steel experiences cycles of heating and cooling. In order to measure the transient mechanical properties at a certain temperature during the quenching process, the steel sample must be able to change temperature quickly to meet the cooling rate requirement of the quenching process and must also stop and stabilize at the preset tensile testing temperature quickly. Traditional heating in electrical radiation furnace can

not meet these requirements. Also for a standard tensile sample, a non-uniform temperature distribution along the gauge length during quick heating and cooling is unavoidable, and this makes it unsuitable to conduct the tensile test on such a standard sample under the conditions of rapid heating and cooling experienced in the process of quenching of steel.

For the tensile test of steel at elevated temperatures during the process of quenching, different approaches must be taken in order to solve the problems discussed above.

It is very important for the entire gauge length to reach the same temperature in the austenitizing stage. The austenite grain size and the dissolution of non-ferrous carbides are greatly affected by the austenite temperature. The grain size has a huge effect on the hardenability of the steel. The rate of carbide precipitation, especially, above (750°C) has a profound effect on the mechanical properties of H13, especially its fracture toughness and thermal cycling durability. So maintaining a close-to-constant temperature along the entire gauge length in the austenitizing stage and during quenching is important in the present study.

The test system must use a different heating and cooling system other than that specified in ASTM E21-05 to develop an appropriate quenching response. ASTM E21-05 assumes a procedure that heats the specimen slowly to the test temperature, holding it there for 20 minutes, and then pulling it to failure at that temperature. Nowhere in E21-05 is there a mention of cooling the sample to an intermediate temperature, and testing it

there, Because of the shoulders, it would be impossible to quench rapidly and establish a uniform temperature in the gauge length quickly. So the E21 standard specimen for an intermediate temperature quenching will probably produce different austenite decomposition products, at different points along the gauge length.

Therefore, to carry out the present work, it is necessary to invent a new type of specimen, it must be able to both heat and cool rapidly, and it must very quickly establish a constant temperature, both during austenitization, and at any prescribed quench temperature.

2.9 Gleeble Thermal –Mechanical Simulator and Resistance Heating

2.9.1 Gleeble Thermal-Mechanical Simulator

Because of the ease of controlling the electrical current, and therefore resistance heating rate, the family of “Gleeble” dynamic thermal-mechanical simulators, developed by Dynamic Systems Inc. [37], uses resistance heating to develop temperature changes in the samples.

In the Gleeble 1500/3500 thermo-mechanical simulators, a 60Hz low voltage but very high current is passed directly through the specimen, so that the resistance of the specimen itself generates the heat by the Joule effect. Since currents of several thousand amperes can be supplied to enable very fast heating rates in a very short time as

encountered in welding, the machines are well suited to simulate welding. One obvious advantage of using self-resistance heating is that the density of the electrical heating current will be relatively uniform across each cross-section, so isothermal transverse planes can be created along the entire specimen and substantially uniform heat generation over the width of a given cross-section can be ensured. This feature of self-resistance heating makes it much better than exterior radiant heating. Also the self-resistance heating can be controlled precisely and instantly by the control of electrical current input using a loop feedback signal based on the measured temperature.

Shown in Figure 2.8 is a photograph of the vacuum chamber in Gleeble 1500 thermo-mechanical simulator, and Figure 2.9 is a schematic illustration of resistance heating of a sample in the Gleeble Machine.

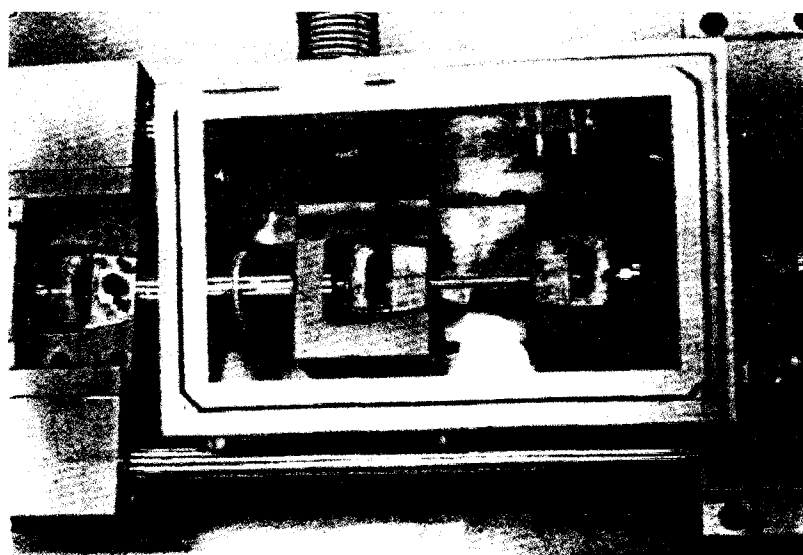


Figure 2.8 Vacuum chamber in Gleeble 1500 simulator.

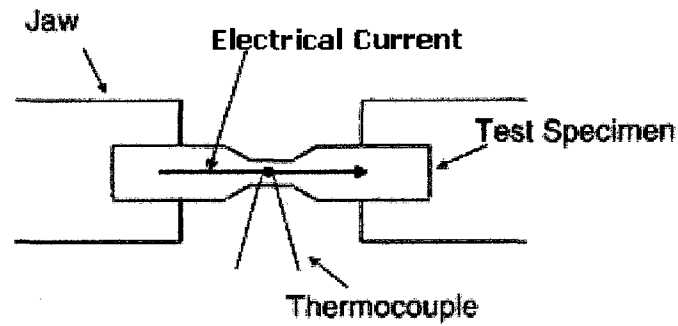


Figure 2.9 Schematic illustration of resistance heating in Gleeble machine

For a resistance heated tensile specimen with varying cross-sections, these cross-sections are connected electrically in series, so they each carry the same total electrical current but at different electrical current densities. Because of this difference in electrical current densities, different heat generation rates will exist for each section. This phenomenon can be quantified through the following calculation on resistance heating.

2.9.2 Resistance heating

Resistance heating is basically the heating of metal when an electrical current flows through it. According to the theory of electricity, the resistant heat generation rate \dot{Q} is proportional to:

$$\dot{Q} = I^2 R \quad (8)$$

where

I is the electric current

R is the resistance

This is called Joule heating or I-squared-R heating effect.

Considering a section of steel with a length of L and a cross section area of A , and assuming all the heat generated by resistance heating while driving a constant electrical current I through it is used to raise its temperature, then the following equation can be established:

$$\dot{Q} \Delta t = C_p M \Delta T \quad (9)$$

where:

C_p is the specific heat of the steel;

M is the mass of the steel.

So the rate of temperature rise will be

$$\frac{\Delta T}{\Delta t} = \frac{\dot{Q}}{C_p M} = \frac{I^2 R}{C_p M} \quad (10)$$

Since the resistance of the steel:

$$R = \beta \frac{L}{A} \quad (11)$$

where β is the resistivity of the steel

and the mass of the steel :

$$M = \rho V = \rho A L \quad (12)$$

Then the temperature change rate can be expressed as follows:

$$\frac{\Delta T}{\Delta t} = \left(\frac{I}{A} \right)^2 \frac{\beta}{C_p \cdot \rho} = \frac{i^2 \beta}{C_p \cdot \rho} \quad (13)$$

It is obvious from the above equation that in a specimen with varying cross-sections:

- The temperature rise rate $\frac{\Delta T}{\Delta t}$ will be proportional to i^2 , the square of the current density $i = \frac{I}{A}$, because the current density will be higher and the heat will be deposited into a smaller mass.
- Much higher heating rate is expected in the sections of small cross-section area because of high current density i there.

In summary, in an adiabatic system, the temperature increase resulting from resistance heating will be inversely proportional to the square of the cross section area, when a constant electrical current is driven through a sample with different cross section areas.

2.9.3 Various Samples Used in Gleeble 1500 Thermo-Mechanical Simulator

Shown in Figure 2.10 is a steel cylinder used in Gleeble machine as a standard sample.

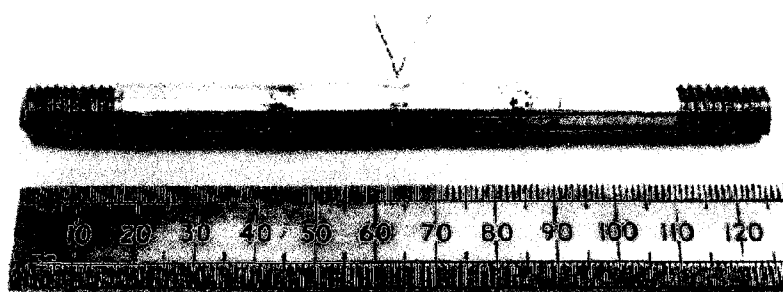


Figure 2.10 Standard sample for Gleeble machine[38]

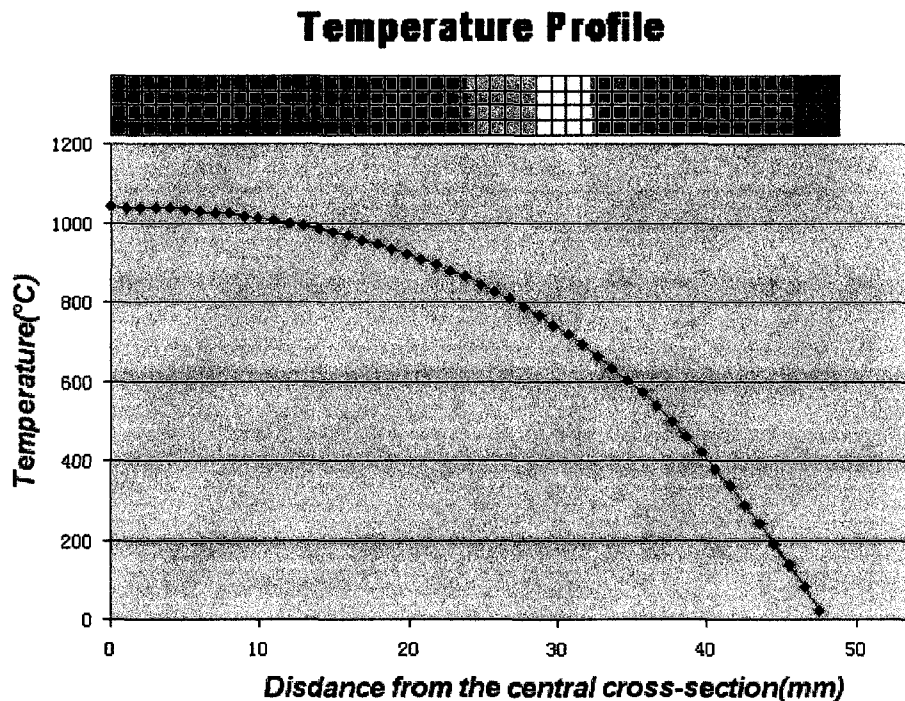


Figure 2.11 The Simulated profile of temperature distribution

When an electrical current is driven through the standard cylinder sample, the resistance heat generation rate will be the same through the whole length of the sample because of the uniform current density through each cross section. But the two ends of the sample

are clamped in grips which are cooled by water. Because of heat loss to the grips through thermal conduction, a non-uniform temperature distribution profile occurs along the gauge length. It is similar to the simulated result by the present author as shown in Figure 2.11. This simulation and all others in this thesis considered heat generation by Joule heating, conduction heat flow and heat loss due to radiation.

For the universally-used standard tensile sample, regardless of the shapes of its cross section, the cross sectional area in the gauge area is designed to be smaller than that of the two ends as shown in Figure 2.12.

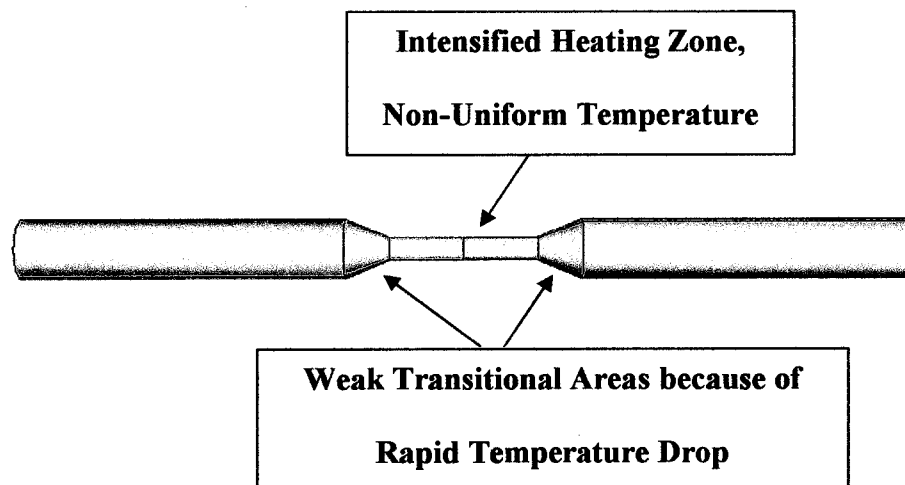


Figure 2.12 Standard tensile sample with varying circular cross section